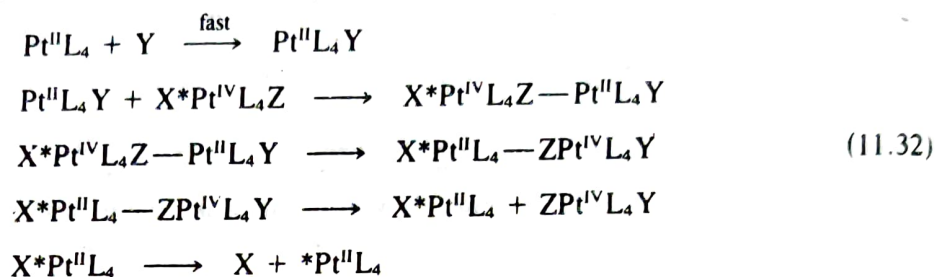


11.6 CATALYSIS OF SUBSTITUTION BY REDOX PROCESSES

Substitutions on octahedral low-spin d^6 complexes proceed quite slowly (see Table 11.13). Pt^{IV} also forms octahedral complexes that undergo slow substitution. In the presence of catalytic amounts of Pt^{II} complexes, however, substitution rates are accelerated by factors of 10^4 – 10^5 . The mechanism of these catalytic reactions is thought to be⁴⁷



In the third step, Pt^{II} is oxidized to Pt^{IV} while the $^*\text{Pt}^{\text{IV}}$ is reduced to $^*\text{Pt}^{\text{II}}$. The two metals exchange roles via a redox process. The relatively fast substitution on Pt^{II} enables the reaction to occur rapidly, and the product $\text{ZPt}^{\text{IV}}\text{L}_4\text{Y}$ contains a metal that originally was Pt^{II} . We also find redox catalysis in $\text{Pd}^{\text{II}}/\text{Pd}^{\text{IV}}$, $\text{Cr}^{\text{II}}/\text{Cr}^{\text{III}}$, and $\text{Ru}^{\text{II}}/\text{Ru}^{\text{III}}$ substitutions where one oxidation state is more labile than the other and substitution on the labile center can be followed by rapid oxidation or reduction to an inert product.

11.7 REDOX REACTIONS

Redox reactions are of wide importance in chemistry. Many classical analytical methods are based on rapid redox reactions, including Fe^{II} determination by titration with HCrO_4^- , as well as oxidations of substances such as $\text{C}_2\text{O}_4^{2-}$ by MnO_4^- . The role of transition metal ions in life processes (see Chapter 18) depends on their ability to participate selectively in electron-transfer reactions. Redox reactions involving two transition-metal complexes generally occur fairly rapidly. Thus, values of E^0 are a rather good guide to the chemistry that actually occurs on a convenient time scale.

Below we consider models for redox reactions of two transition-metal-containing complexes. Oxidations of nonmetallic species by metallic ions have been reviewed.⁴⁸

11.7.1 Inner- and Outer-Sphere Reactions

Two models for redox mechanisms of metal complexes currently are considered operative. In the **inner-sphere mechanism**, the coordination spheres of the two metals interpenetrate in the transition state. A bridging ligand is coordinated to both the oxidant and the

⁴⁷ W. R. Mason, *Coord. Chem. Rev.* 1972, 7, 241.

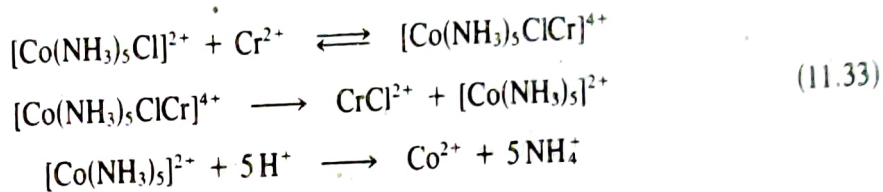
⁴⁸ A. McAuley, *Coord. Chem. Rev.* 1970, 5, 245; J. K. Beattie and G. P. Haight, *Prog. Inorg. Chem.* 1972, 17, 93; D. Benson, "Mechanisms of Oxidation by Metal Ions," in *Reaction Mechanisms in Organic Chemistry*, Vol. 10, Elsevier, New York, 1976.

reductant and forms part of the first coordination sphere of each. In the **outer-sphere mechanism**, each separate coordination sphere remains intact.

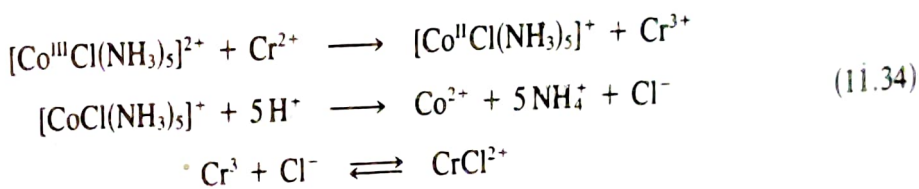
The first definitive evidence for an inner-sphere process was provided by Taube and Myers, who investigated the Cr^{2+} reduction of $[\text{Co}(\text{NH}_3)_5\text{Cl}]^{2+}$.⁴⁹

The final products in acid solution are Co^{2+} , Cr^{3+} , CrCl^{2+} , Cl^- , and NH_4^+ . It is possible to imagine both inner- and outer-sphere mechanisms that would lead to these products.

Inner Sphere



Outer Sphere



However, the inner-sphere pathway must be operative, because Cr^{3+} is inert to substitution on the time scale for the reaction. At 25°C , the second-order rate constant for Cl^- anation of Cr^{3+} is $2.9 \times 10^{-8} \text{ M}^{-1} \text{ s}^{-1}$, whereas that for reduction is $6 \times 10^3 \text{ M}^{-1} \text{ s}^{-1}$. Hence, the CrCl^{2+} could not have arisen by substitution with free Cl^- on the time scale required to separate the products. The electron-transfer step converts labile Cr^{2+} into substitution-inert Cr^{III} , which retains the bridging chloride in its coordination sphere when the bridged species breaks up. Notice also that Cr^{2+} is sufficiently labile ($k_{\text{exch}} \sim 10^8 \text{ s}^{-1}$ at 25°C) that substitution of the bridging Cl^- into its coordination sphere is not rate-limiting.

A sufficient condition for establishing that a reaction is inner-sphere is that one product be substitution-inert and retain the bridging ligand originally coordinated to the other reactant. This means that the oxidant and reductant must be chosen so that one is inert while the other is labile and the products are labile and inert in the opposite sense. Rather few inner-sphere reactions fulfill this requirement (that is, the condition is not a necessary one). Later, we shall devote attention to other ways of deciding whether a reaction is inner-sphere.

The above discussion reveals that a sufficient condition for the outer-sphere mechanism is that the redox rate be much faster than substitution on either metal center. An example is the reduction of $[\text{RuBr}(\text{NH}_3)_5]^{2+}$ by V^{2+} . The second-order rate constant for the reduction is $5.1 \times 10^3 \text{ M}^{-1} \text{ s}^{-1}$, whereas aquation reactions on Ru^{III} and V^{II} centers have first-order rate constants of 20 and 40 s^{-1} , respectively.

Before discussing other ways of assigning mechanism, we review some general features of outer- and inner-sphere reactions.

⁴⁹In discussing redox reactions, M^{n+} ordinarily is taken to represent the metal ion with its first coordination sphere occupied by aqua ligands. Thus $\text{Cr}^{2+} \equiv [\text{Cr}(\text{H}_2\text{O})_6]^{2+}$. ML^{n+} represents the complex in which one aqua ligand is replaced by L.

► 11.7.2 Marcus Theory

Marcus⁵⁰ has calculated from theory the contributions to ΔG^\ddagger for outer-sphere reactions; this work won him the 1992 Nobel prize in chemistry. In his model, outer-sphere reactions are regarded as involving five steps:

1. Reactants diffuse together to form an outer-sphere complex in which both metal coordination spheres remain intact.
2. Bond distances around each metal change to become more "productlike".
3. The solvent shell around the outer-sphere complex reorganizes.
4. The electron is transferred.
5. The products diffuse away; this step is generally fast.

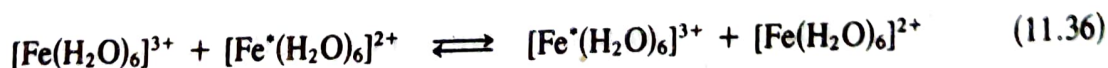
Calculation of contributions by the various steps to ΔG^\ddagger can be achieved because no bond breaking is involved. Marcus⁵⁰ showed that

$$\Delta G^\ddagger = \Delta G_{\text{inner sphere}}^\ddagger + \Delta G_{\text{solvation}}^\ddagger + \frac{\Delta G_r^0}{2} + \frac{(\Delta G_r^0)^2}{16(\Delta G_{\text{inner sphere}}^\ddagger + \Delta G_{\text{solvation}}^\ddagger)} \quad (11.35)$$

where ΔG_r^0 is the overall free-energy change for the reaction corrected for the work required to bring the reactants to the distance r where redox occurs, $\Delta G_{\text{inner sphere}}^\ddagger$ is the energy required for changing bond lengths, and $\Delta G_{\text{solvation}}^\ddagger$ is the solvent reorganization energy. We now discuss each of these contributions in more detail with a view toward understanding the factors involved in each rather than with the goal of actually calculating these terms ourselves.

ΔG^0 , the overall free-energy change, is easily calculated from reduction potentials: $-\Delta G^0 = RT \ln K_{\text{eq}} = nFE^0$. The work involved in bringing reactants together is just $U(r)$, where $U(r)$ is the sum of attractive and repulsive potentials for complex ions as they approach. $U(r)$ is involved in the calculation of K for outer-sphere complex formation and is defined in the footnote to Table 11.14. $\Delta G_r^0 = \Delta G^0 + NU(r)$.

$\Delta G_{\text{inner sphere}}^\ddagger$ results from bond length changes occurring in the separate coordination spheres of the outer-sphere complex before electron transfer can happen. We first consider why such changes are necessary. A well-known outer-sphere reaction is the so-called **self-exchange**; for example,



The equilibrium constant for this reaction is 1 and $\Delta G^0 = 0$; hence, $\Delta G^\ddagger \approx \Delta G_{\text{inner sphere}}^\ddagger + \Delta G_{\text{solvation}}^\ddagger$. The measured value of k is $4 \text{ M}^{-1} \text{ s}^{-1}$ at 25°C . Before an electron can be transferred, the Fe—O bond lengths must distort. Those of the Fe^{3+} complex lengthen to a distance halfway between the Fe^{2+} and Fe^{3+} distances. Those of the Fe^{2+} complex contract to the same distance. This requires energy expenditure. This model for the outer-sphere process is in accord with the **Franck–Condon principle**, which states

⁵⁰R. A. Marcus, *Annu. Rev. Phys. Chem.*, **1964**, *15*, 155; T. W. Newton, *J. Chem. Educ.*, **1968**, *45*, 571.

that electron transfer is much faster than nuclear motion. As far as electrons are concerned, nuclear positions are frozen during the time period required for electron transfer.

If this reorganization energy (Franck–Condon energy) were not expended, initial products of self-exchange would be (a) $[^*\text{Fe}(\text{H}_2\text{O})_6]^{3+}$ with bond distances characteristic of $[\text{Fe}(\text{H}_2\text{O})_6]^{2+}$ and (b) $[\text{Fe}(\text{H}_2\text{O})_6]^{2+}$ with bond distances characteristic of $[\text{Fe}(\text{H}_2\text{O})_6]^{3+}$. The energy released when these species relax to their stable geometries would be created from nothing, in violation of the first law of thermodynamics.

The reaction profile⁵¹ for self-exchange is shown in Figure 11.15a. The energy is the total energy for a pair of ions in the outer-sphere complex. The reaction coordinate represents all changes in bond lengths and angles in the coordination spheres for the pair of complex ions. The curve is symmetric, since products and reactants are identical. In this picture, electron transfer occurs where the energy curve for products intersects that for reactants; this occurs at some value of the coordinate for which energy is not a minimum. As the reaction coordinate approaches its transition-state value, the wavefunctions for reactants and products mix, creating two separate energy states instead of the parabolas crossing. Dashed lines show the course of the parabolas if no mixing occurred; and the distance between the two solid curves ($2H_{AB}$) is a measure of the degree of mixing. The path of the self-exchange is the motion of a point from the reactant well up the Franck–Condon barrier and on down into the product well.

$\Delta G_{\text{inner sphere}}^\ddagger$ is usually calculated by using the expression

$$\Delta G_{\text{inner sphere}}^\ddagger = \frac{3Nf_{\text{av}}(\Delta d)^2}{8} \quad (11.37)$$

where Δd is the change in M—L distance on going from the ground to the transition state and f_{av} is the average value of the force constant for the symmetric breathing vibrational mode by which bond-length changes are considered to be achieved.

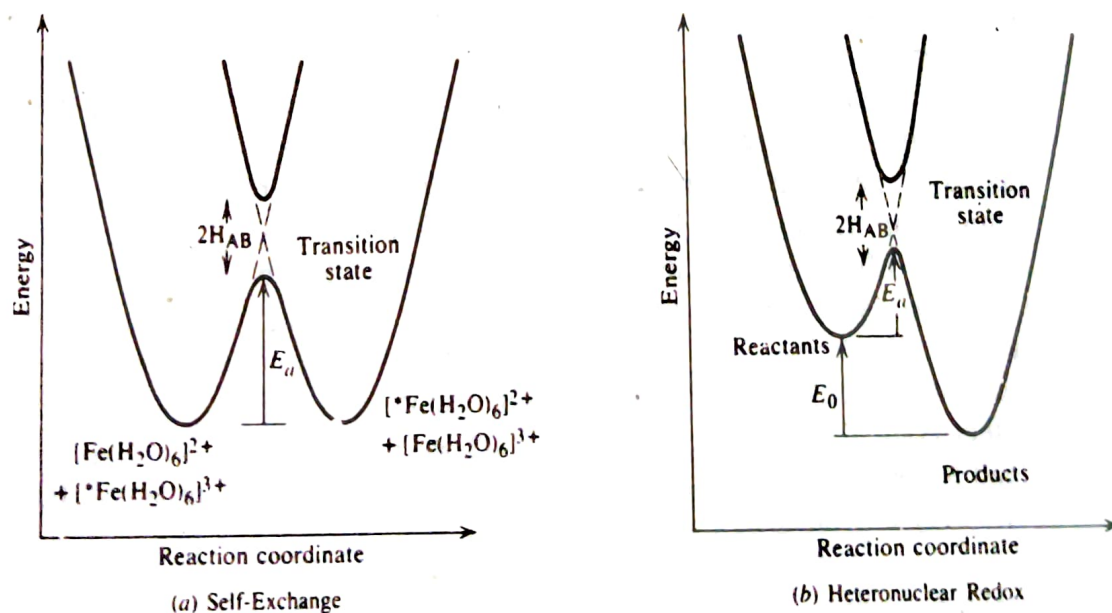


Figure 11.15 Reaction profiles for outer-sphere redox reactions.

⁵¹N. A. Lewis, *J. Chem. Educ.* 1980, 57, 478.

$\Delta G_{\text{solvation}}^{\ddagger}$ can be calculated from the expression

$$\Delta G_{\text{solvation}}^{\ddagger} = N \frac{\Delta e^2}{4} \left(\frac{1}{2a_1} + \frac{1}{2a_2} - \frac{1}{r} \right) \left(\frac{1}{n^2} - \frac{1}{D} \right) \quad (11.38)$$

where Δe is the charge transferred from one metal the other, a_1 and a_2 are the ground-state radii of the complexes, r is the separation between the metals in the transition state (often taken as $a_1 + a_2$), n is the refractive index of the medium and D is the dielectric constant of the medium. This calculation assumes that the solvent is a dielectric continuum instead of consisting of individual molecules.

Values of k are calculated from the formula⁵²

$$k \sim \frac{4\pi N r^3}{3000} \kappa_{\text{el}} \nu_n e^{-\Delta G^{\ddagger}/RT} \quad (11.39)$$

$$\sim K_{\text{os}} \kappa_{\text{el}} \nu_n e^{-(\Delta G^{\ddagger}_{\text{inner sphere}} + \Delta G^{\ddagger}_{\text{solvation}} + 0.5\Delta G^0)/RT}$$

where κ_{el} is the so-called **electron transmission coefficient** and represents the probability of electron transfer at the transition-state geometry. For reactions in which there is strong interaction between the reactant and product wavefunctions, a large energy gap ($2H_{\text{AB}}$) exists between the solid curves of Figure 11.15a; the system stays on the lower-energy curve and passes smoothly from reactants to products. Such systems are called **adiabatic** and $\kappa_{\text{el}} = 1$. When coupling is small, $2H_{\text{AB}}$ is small and the reactant system may reach the transition state which is the intersection of reactant and product energy curves and continue on up the reactant parabola (and roll back down) without executing the transition to products. In such nonadiabatic systems, $\kappa_{\text{el}} \ll 1$. In calculations, κ_{el} is taken as = 1. ν_n is a nuclear frequency factor and represents the frequency of a vibrational mode between the two metal atoms which removes the system from its transition-state geometry; it is often taken to be $1 \times 10^{13} \text{ s}^{-1}$. K_{os} is the outer-sphere complex formation constant.

Table 11.23 compares some calculated and observed values for self-exchange rate constants. The agreement is good for Fe and Co, but not for $\text{Ru}^{3+/2+}$. In cases where k_{calc} is much greater than k_{obs} , the difference is usually attributed to nonadiabaticity. A number of approximations are involved in calculations beyond those made in the theory. For instance, it is not clear what the bond distances in the transition state are; Δd is usually estimated as the difference between bond distances in the reduced and oxidized forms of the couple, but this may not be correct. Also, force constants for symmetric breathing vibrations are often not available, and so on. However, we can see some important trends. Complexes with larger estimated values of Δd have higher $\Delta G^{\ddagger}_{\text{inner sphere}}$ and lower k . Electron transfer from $e_g \sigma^* \rightarrow t_{2g} \pi$ leads to larger Δd (compare Co complexes with others). Bond-length changes are especially important because $\Delta G^{\ddagger}_{\text{inner sphere}}$ depends on $(\Delta d)^2$; this effect contributes to the small values for self-exchange of Co complexes. Larger ligands lead to smaller $\Delta G^{\ddagger}_{\text{solvation}}$ and larger k , all other things being equal. (Compare NH_3 , en, and bipy complexes.)

⁵² This formula is approximate and holds when

$$\Delta G_r^{02} < (\Delta G^{\ddagger}_{\text{inner sphere}} + \Delta G^{\ddagger}_{\text{solvation}})$$

This will certainly be the case for self-exchange when $\Delta G^0 = 0$ and for reactions where ΔG^0 is small.

Table 11.23 Calculation of self-exchange constants for redox couples^a

| | $Fe^{3+.2+}$ | $Ru^{3+.2+}$ | $Ru(NH_3)_6^{3+.2+}$ | $Ru(bipy)_3^{3+.2+}$ | $Co(NH_3)_6^{3+.2+}$ | $Co(en)_3^{3+.2+}$ | $Co(bipy)_3^{3+.2+}$ |
|--|--------------|-----------------|----------------------|----------------------|-----------------------|----------------------|----------------------|
| E^0 (volts): | +0.74 | +0.045 | +0.051 | +1.26 | +0.058 | -0.24 | — |
| r (pm): | 65 | 65 | 67 | 136 | 66 | 84 | 136 |
| $K_{os}/10^{-1} M$: | 0.05 | 0.33 | 1.0 | 3.3 | 0.33 | 1.2 | 3.3 |
| $\Delta G_{inner\ sphere}^\ddagger$ (kJ/mol): | 35.2 | 15.9 | 3.3 | 0 | 73.7 | — | 57.3 |
| $\Delta G_{solvation}^\ddagger$ (kJ/mol): | 28.9 | 28.9 | 28.0 | 13.8 | 28.5 | 5.3 | 13.8 |
| Δd (pm): | 1.3 | 0.9 | 0.2 | 0.0 | 2.2 | 2.1 | 1.9 |
| k_{calc} ($M^{-1} s^{-1}$): | 3 | 4×10^3 | 1×10^5 | 1×10^9 | 4.8×10^{-6b} | 2×10^{-5b} | 20 |
| k_{obs} ($M^{-1} s^{-1}$): | 4 | 50 | 2.8×10^4 | 4.2×10^8 | 8×10^{-6} | 7.7×10^{-5} | 18 |

^a Data from B. S. Braunschweig, C. Creutz, D. H. Macartney, T. -K. Sham, and N. Sutin, *Disc. Faraday Soc.* **1982**, 74, 113; R. A. Marcus and N. Sutin, *Biochem. Biophys. Acta* **1985**, 811, 265.

^b A. Hammershor, D. Geselowitz, and H. Taube, *Inorg. Chem.* **1984**, 23, 979.

► 11.7.3 Heteronuclear Redox Reactions and Simplified Marcus Theory

Most redox reactions of interest are heteronuclear—they involve two different metals. Nevertheless, each metal complex must undergo separately the kind of rearrangement described above. Thus, we might expect that $\Delta G_{\text{inner sphere}}^\ddagger$ for the heteronuclear reaction will be related to $\Delta G_{\text{inner sphere}}^\ddagger$ for self-exchange of each of the reactants. Figure 11.15b shows a reaction profile for a heteronuclear redox reaction that is thermodynamically favorable. The activation barrier height depends on the relative placement of reactant and product potential energy curves—which is equivalent to saying that the value of the rate constant also depends on the overall free-energy change ΔG^0 .

A simplified version of the Marcus equation which incorporates these considerations is

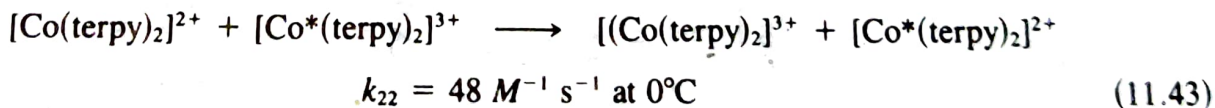
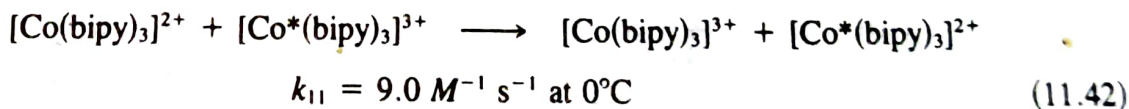
$$k_{12} = \sqrt{k_{11}k_{22}K_{12}f_{12}} \quad (11.40)$$

where

$$\log f_{12} = \frac{(\log K_{12})^2}{4 \log \frac{k_{11}k_{22}}{Z^2}} \quad (11.41)$$

and Z is the number of collisions per second between particles in solution ($\sim 10^{11} \text{ M}^{-1} \text{ s}^{-1}$ at 25°C). The Marcus equation shows that rates of redox reactions depend on an intrinsic factor (through k_{11} and k_{22}) and a thermodynamic factor (through K_{12}). The rate is related to the driving force, and more thermodynamically favorable reactions are faster. This equation is an example of a linear free-energy relationship.

One use of the simplified Marcus equation is to predict the outer-sphere rate constant for a cross-reaction. To predict k_{12} for reduction of $[\text{Co}(\text{bipy})_3]^{3+}$ by $[\text{Co}(\text{terpy})_2]^{2+}$, we require self-exchange constants.



Reduction potentials for $[\text{Co}(\text{terpy})_2]^{3+}$ and $[\text{Co}(\text{bipy})_3]^{3+}$ are +0.31 and +0.34 V, respectively. Hence, $\log K_{12} = 0.553$ and $K_{12} = 3.57$.

$$\log f_{12} = \frac{(0.553)^2}{4 \log \frac{9.0 \times 48.0}{10^{22}}} = -3.95 \times 10^{-3}, \quad f_{12} = 0.99 \quad (11.44)$$

$$k_{12} = \sqrt{(9.0 \text{ M}^{-1} \text{ s}^{-1})(48.0 \text{ M}^{-1} \text{ s}^{-1})(3.57)(0.99)} = 39 \text{ M}^{-1} \text{ s}^{-1}$$

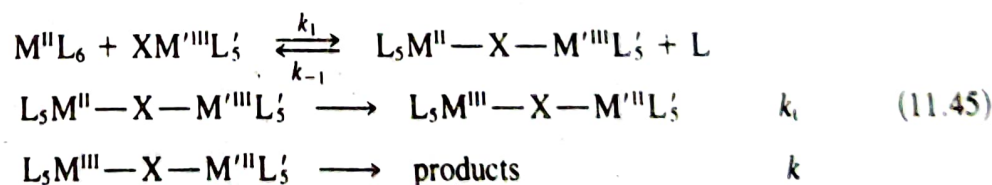
This calculated value compares favorably with the measured value of $64 M^{-1} s^{-1}$.⁵³ Agreement between calculated and measured rate constants generally is good as long as the driving force is not too great ($K \leq 10^6$; $f \geq 0.2$); it has been estimated⁵⁴ that rate constants can be calculated to within a factor of ~ 25 . Data in Table 11.24 are fairly typical. In the case of an unknown mechanism, agreement between the observed rate constant and that calculated from the Marcus equation is regarded as evidence for an outer-sphere pathway.⁵⁴

Self-exchange rates can also be calculated from the simplified Marcus equation. Some values calculated for $Ru^{2+/3+}$ self-exchange are shown in Table 11.25; the agreement with the measured value of $50 M^{-1} s^{-1}$ is within a factor of ten for all cases, and the average is $\sim 40 M^{-1} s^{-1}$. Calculations of this sort have been employed to estimate self-exchange rates which cannot be easily measured directly—for example, in metalloproteins.

Self-exchange constants calculated for $Fe^{3+/2+}$ in this way usually turn out to be orders of magnitude smaller than the measured one (Table 11.26). It has been suggested that a value of $\sim 10^{-3}$ for the Fe self-exchange would lead to better agreement with experiment. One interpretation is that the measured exchange rate is really that for inner-sphere electron transfer. Some evidence in favor of this view is that the calculated $\Delta G_{\text{inner sphere}}^\ddagger$ is much larger for Fe than for Ru, which leads to the expectation that k_{11} for Fe should be orders of magnitude lower than that for Ru. Also, $V^{2+/3+}$, where $\Delta d \sim 1.5$ pm compared to 1.3 for Fe, has $k_{11} = 1.1 \times 10^{-2} M^{-1} s^{-1}$. However, recent measurement⁵⁵ of ΔV^\ddagger suggests that Fe self-exchange is indeed outer-sphere. It may be that heterometallic electron transfers involving Fe exhibit nonadiabaticity which is absent in the self-exchange.

► 11.7.4 Inner-Sphere Reactions

A generalized mechanism for inner-sphere electron-transfer reactions involves three separate steps:



The first involves substitution by the bridging group X into the coordination sphere of the labile reactant (usually the reductant⁵⁶) to form the **precursor complex**. The precursor complex then undergoes the same kind of reorganization described for outer-sphere pathways, followed by electron transfer to give the **successor complex**. Thus, events in this step are related to those in outer-sphere reactions. In the last step the successor complex

⁵³ R. Farina and R. G. Wilkins, *Inorg. Chem.* **1968**, *7*, 514.

⁵⁴ For a critical review of the applicability of the Marcus equation, see M. Chou, C. Creutz, and N. Sutin. *J. Am. Chem. Soc.* **1977**, *99*, 5615.

⁵⁵ W. H. Jolly, D. Stranks, and T. W. Swaddle, *Inorg. Chem.* **1990**, *29*, 1948.

⁵⁶ The bridging ligand may be carried by the reductant, as in the $[Fe(CN)_6]^{4-}$ reduction of $HCrO_4^-$.

Table 11.24 Comparison between calculated and observed rate constants for outer-sphere reactions^a

| Reaction | k_{12} obsd. ($M^{-1} s^{-1}$) | k_{12} calcd. ($M^{-1} s^{-1}$) | k_{11} ($M^{-1} s^{-1}$) | k_{22} ($M^{-1} s^{-1}$) | $E^0 V(K_{12})$ | f |
|---------------------------------------|---------------------------------------|--|---------------------------------|---------------------------------|-------------------------------|----------------------|
| $[Fe(CN)_4]^{4-} - [IrCl_6]^{2-}$ | 3.8×10^5 | 1×10^6 | 7.4×10^2 | 2.3×10^5 | 0.24(1.2×10^4) | 5.1×10^{-1} |
| $[Fe(CN)_6]^{4-} - [Fe(phen)_3]^{3+}$ | $>10^8$ | $>1 \times 10^8$ | 7.4×10^2 | $>3 \times 10^7$ | 0.39(3.5×10^6) | 1.2×10^{-1} |
| $[Fe(CN)_6]^{4-} - MnO_4^-$ | 1.7×10^5 | 6×10^4 | 7.4×10^2 | 3×10^3 | 0.20(2.5×10^3) | 6.6×10^{-1} |
| $[Fe(CN)_6]^{4-} - Ce^{IV}$ | 1.9×10^6 | 6×10^6 | 7.4×10^2 | 4.4 | 0.76(5.8×10^{12}) | 4.7×10^{-3} |
| $[Fe(phen)_3]^{2+} - Ce^{IV}$ | 1.4×10^5 | $>7 \times 10^6$ | $>3 \times 10^7$ | 4.4 | 0.36(1.1×10^6) | 2.1×10^{-1} |
| $[Fe(phen)_3]^{2+} - MnO_4^-$ | 6.1×10^3 | >3 | $>3 \times 10^7$ | 3×10^3 | -0.50(3.4×10^{-9}) | 2.4×10^{-2} |
| $Fe^{2+} - [Fe(phen)_3]^{3+}$ | 3.7×10^4 | $>5 \times 10^6$ | 4.0 | $>3 \times 10^7$ | 0.35(7.6×10^5) | 2.4×10^{-1} |
| $Fe^{2+} - Ce^{IV}$ | 1.3×10^6 | 5×10^5 | 4.0 | 4.4 | 0.71(8.3×10^{11}) | 2.0×10^{-2} |
| $Fe^{2+} - [IrCl_6]^{2-}$ | 3.0×10^6 | 2×10^4 | 4.0 | 2.3×10^5 | 0.16(5.0×10^2) | 8.9×10^{-1} |
| $Cr^{2+} - Fe^{3+}$ | 2.3×10^3 | $<1 \times 10^6$ | $\leq 2 \times 10^{-5}$ | 4.0 | 1.18(6.6×10^{19}) | 1.7×10^{-4} |

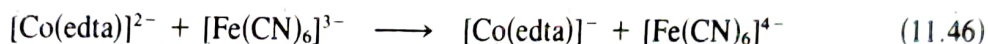
^a From D. A. Pennington, in *Coordination Chemistry*, Vol. 2, A. E. Martell, Ed., American Chemical Society, Washington, D.C., 1978.
 k_{11} and k_{22} are the rate constants for self-exchange for reductant and oxidant, respectively, for the given redox pair.

Table 11.25 Calculated self-exchange rate constants for $\text{Ru}^{3+/2+}$ using Equation (11.40)^a

| Cross-reaction | K_{12} | k_{12}^{obs} | k_{22}^{obs} | k_{11}^{calc} |
|---|-------------------|-----------------------|-----------------------|------------------------|
| $\text{Ru}^{3+} + \text{V}^{2+}$ | 5.8×10^7 | 2.5×10^2 | 1.5×10^{-2} | 0.43 |
| $\text{Ru}^{3+} + [\text{Ru}(\text{NH}_3)_6]^{2+}$ | 6×10^2 | 1.4×10^4 | $\sim 3 \times 10^3$ | 140 |
| $[\text{Co}(\text{phen})_3]^{3+} + \text{Ru}^{2+}$ | 4.2×10^2 | 53 | ~ 40 | 0.20 |
| $[\text{Ru}(\text{NH}_3)_5\text{py}]^{3+} + \text{Ru}^{2+}$ | 35 | 1.1×10^4 | 4.7×10^5 | 8.0 |

^aData from J. T. Hupp and M. J. Weaver, *Inorg. Chem.* **1983**, 22, 2557 and M. J. Weaver and E. L. Yee, *Inorg. Chem.* **1980**, 19, 1936 and references therein.

breaks up to give the products. If M^{III} is inert to substitution and M'^{III} is labile, transfer of the bridging ligand occurs, affording $\text{M}^{\text{III}}\text{XL}_5$ as one product—which provides evidence of the inner-sphere mechanism. This is not always the case, however. For example, in Reaction (11.46) no ligand transfer occurs, since both Fe complexes are inert.



In principle, any one of the three steps could be rate-determining. Figure 11.16 shows potential-energy diagrams corresponding to each possibility.

Type I. Most inner-sphere redox reactions correspond to the case in which the electron-transfer step (with attendant bond-length and solvation changes) that transforms the precursor into the successor complex is slowest. ($k_{\text{et}} \ll k_1, k_{-1}$ and k) All the inner-sphere reactions mentioned so far are examples of this type. Inner-sphere redox reactions are placed in this class if no evidence exists for assigning them to the other types. For these reactions $k_{\text{obs}} = Kk_{\text{et}}$, where $K = k_1/k_{-1}$ is the equilibrium constant for precursor complex formation and k_{et} is the rate constant for e transfer defined in Equations (11.45).

Because the e -transfer step involves a reorganization barrier similar to the outer-sphere case, a Marcus-type relationship applies k_{et} . The study of dinuclear complexes such as $\left[(\text{bipy})_2\text{ClRu}^{\text{II}} - \text{N} \begin{array}{c} \diagup \diagdown \\ \diagdown \diagup \\ \diagup \diagdown \end{array} \text{N} - \text{Ru}^{\text{III}}(\text{bipy})_2\text{Cl} \right]^{3+}$ as model systems for inner-sphere precursor complexes has enabled evaluation of Franck-Condon barriers, solvation ener-

Table 11.26 Calculated^a self-exchange rate constants for $\text{Fe}^{3+/2+}$ using Equation (11.40)

| Cross-reaction | K_{12} | k_{12}^{obs} | k_{22}^{obs} | k_{11}^{calc} |
|---|-------------------|-----------------------|-----------------------|------------------------|
| $\text{Fe}^{3+} + \text{Ru}^{2+}$ | 5×10^8 | 2.3×10^3 | 50 | 1.4×10^{-3} |
| $\text{Fe}^{3+} + [\text{Ru}(\text{NH}_3)_5\text{py}]^{2+}$ | 1.5×10^7 | 5.8×10^4 | 4.7×10^5 | 2.3×10^{-3} |
| $\text{Fe}^{3+} + [\text{Ru}(\text{NH}_3)_4\text{bipy}]^{2+}$ | 4.5×10^3 | 7.2×10^3 | $\sim 1 \times 10^7$ | 2×10^{-3} |
| $[\text{Fe}(\text{bipy})_3]^{3+} + \text{Fe}^{2+}$ | 1.2×10^5 | 3.7×10^4 | $\sim 1 \times 10^9$ | 4×10^{-6} |

^aData from J. T. Hupp and M. J. Weaver, *Inorg. Chem.* **1983**, 22, 2557 and M. J. Weaver and E. L. Yee, *Inorg. Chem.* **1980**, 19, 1936 and references therein.

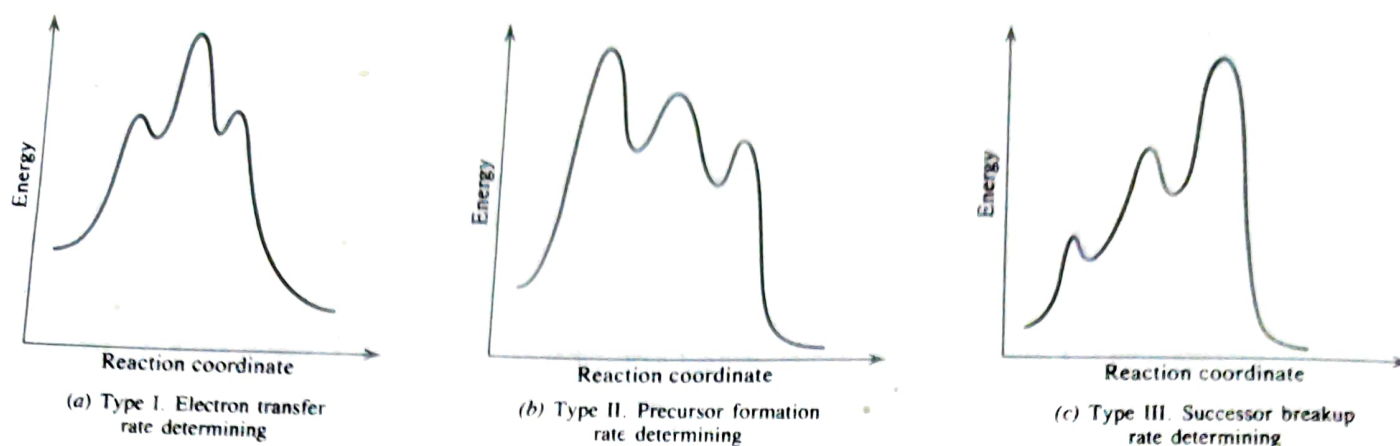


Figure 11.16 Reaction profiles for inner-sphere redox reactions. (From R. G. Linck, in *M. T. P. International Review of Science, Chemistry*, Vol. 9, series one, M. L. Tobe, Ed., University Park Press, Baltimore, 1972.)

gies, and so on.⁵⁷ Reaction profiles such as those shown in Figure 11.15 are applicable to the *e*-transfer step in inner-sphere reactions.

Type II. When formation of the precursor complex is rate-determining (Figure 11.16b), the reaction rate is controlled by the substitution rate into the coordination sphere of the labile reactant ($k_1 \ll k_{et}, k$). Table 11.27 gives kinetic parameters for some reductions by V^{2+} which are substitution-controlled. The reduction rates are quite similar, and the kinetic parameters closely match those for substitution on V^{2+} . For water exchange on V^{2+} , $k = 100 \text{ s}^{-1}$, $\Delta H^\ddagger = 68.6 \text{ kJ/mol}$, and $\Delta S^\ddagger = -23 \text{ J/mol K}$. For NCS^- substitution, $k = 28 \text{ M}^{-1} \text{ s}^{-1}$, $\Delta H^\ddagger = 56.5 \text{ kJ/mol}$, and $\Delta S^\ddagger = -29 \text{ J/mol K}$. That the rates should be so similar for a variety of possible bridging ligands could be interpreted on an outer-sphere model. However, the similarity of the activation parameters to those for substitution is evidence that the process is controlled by the dissociative activation of the substitution (see Section 11.3.4).

Table 11.27 Rate parameters for some reductions by V^{2+} at 25°C^a

| Oxidant | $k \text{ (M}^{-1} \text{ s}^{-1}\text{)}$ | $\Delta H^\ddagger \text{ (kJ/mol)}$ | $\Delta S^\ddagger \text{ (J/mol K)}$ |
|--|--|--------------------------------------|---------------------------------------|
| $[\text{Co}(\text{NH}_3)_5\text{C}_2\text{O}_4\text{H}]^{2+}$ | 12.5 | 51.0 | -54 |
| $[\text{Co}(\text{NH}_3)_5\text{C}_2\text{O}_4]^+$ | 45.3 | — | — |
| <i>cis</i> - $[\text{Co}(\text{NH}_3)(\text{en})_2(\text{N}_3)]^{2+}$ | 10.3 | 52.7 | -50 |
| <i>cis</i> - $[\text{Co}(\text{H}_2\text{O})(\text{en})_2(\text{N}_3)]^{2+}$ | 16.6 | 50.6 | -50 |
| <i>trans</i> - $[\text{Co}(\text{en})_2(\text{N}_3)_2]^+$ | 26.6 | 51.0 | -46 |
| <i>trans</i> - $[\text{Co}(\text{H}_2\text{O})(\text{en})_2(\text{N}_3)]^{2+}$ | 18.1 | 46.0 | -67 |
| Cu^{2+} | 26.6 | 46.7 | -57.7 |

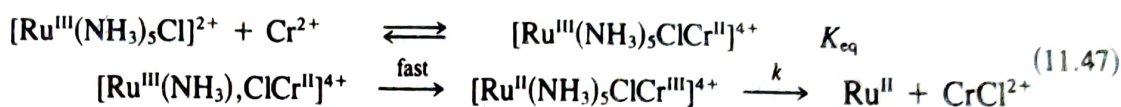
^a From the work of Taube, Espenson, Sutin, Linck, and others.

⁵⁷ T. J. Meyer, *Acc. Chem. Res.* 1978, 11, 94.

A corollary of these considerations is that any V^{2+} reduction with a rate constant substantially in excess of the substitution rate constant must be outer-sphere (e.g., the Fe^{3+} reduction for which $k_{12} = 1.8 \times 10^4 M^{-1} s^{-1}$).

Substitution-controlled reductions by Cr^{2+} , Fe^{2+} , Cu^+ , and Eu^{2+} are known.

Type III. You might expect the breakup of the successor complex to be rate-determining ($k \ll k_{et}$) when the electron configuration of both metals in the successor complex leads to substitution inertness. Usually, the existence of a binuclear complex in equilibrium with reactants is indicated by the form of the rate law—as, for example, in the Cr^{2+} reduction of $[Ru(NH_3)_5Cl]^{2+}$. A complex having both Ru and Cr is kinetically detectable. Because the successor complex would contain inert Ru^{II} and Cr^{III} , we assume that this must be the species detected.⁵⁸ The mechanism involved is



This is consistent with the observed rate law

$$-\frac{d}{dt}[Ru^{III}] = \frac{kK_{eq}}{1 + K_{eq}[Cr^{2+}]} [Ru^{III}]_0 [Cr^{2+}] \quad (11.48)$$

which you should verify as an exercise.⁵⁹

Sometimes successor complexes are sufficiently stable that they can be prepared independently and their breakup followed. An example is the successor complex from the reduction of VO^{2+} by V^{2+} : $[V^{III}(OH)_2V^{III}]^{4+}$ ⁶⁰; this species can also be prepared by hydrolysis of V^{III} solutions. Comparatively few redox reactions have been shown to belong to Type III.

The Bridging Ligand

Even in reactions in which precursor complex formation is not rate-determining, the nature of the bridging ligand can be quite important because the activation barrier for precursor formation may represent a substantial fraction of the overall activation energy and because electron transfer is mediated by the bridging ligand. This section points out some aspects of the role of the bridging ligand and their mechanistic consequences.

If a ligand is to function in a bridging capacity, an unshared pair of sufficiently basic electrons is required. Thus, complexes such as $[Co(NH_3)_6]^{3+}$ and $[Co(NH_3)_5(py)]^{3+}$ react only via outer-sphere paths. Current evidence also indicates that unshared pairs on water

⁵⁸It is true that the mere detection of a bridged species does not mean that it is involved in the redox reaction. Other evidence, including comparison with related systems, is needed to establish this point. See, for example, L. Rosenheim, D. Speiser, and A. Haim, *Inorg. Chem.* **1974**, *13*, 1571; D. H. Huchital and J. Lepore, *Inorg. Chem.* **1978**, *17*, 1134.

⁵⁹*Hint:* Rate = $k_{obs} [Cr^{2+}][Ru^{III}]_0$, where $[Ru^{III}]_0$ represents the concentration of $[RuCl(NH_3)_5]^{2+}$ used in preparing the reacting solution. However, this is now partitioned between two solution species, $[RuCl(NH_3)_5]^{2+}$ and the Ru—Cr dimer. Cr^{2+} is assumed present in large excess.

⁶⁰T. W. Newton and F. B. Baker, *Inorg. Chem.* **1964**, *3*, 569; L. Pajdowski and B. Jezowska-Trzebiatowska, *J. Inorg. Nucl. Chem.* **1966**, *28*, 443.

are not sufficiently basic to allow aqua complexes an inner-sphere path.

Evidence for an inner-sphere mechanism follows in selected cases from changes in rate as a function of bridging ability of ligands. Table 11.28 contains rate data for some reductions as the possible bridging ligand is changed from H_2O to OH^- and from N_3^- to NCS^- . The $[\text{Ru}(\text{NH}_3)_6]^{2+}$ reductions must be outer-sphere (*o.s.*) because the reductant is both inert to substitution on the time scale of the redox reaction and without electron pairs for bridging. The rates of reaction with aqua and hydroxo complexes are quite similar. The large rate enhancement on going from H_2O to OH^- complexes when Cr^{2+} is the reductant supplies strong evidence that OH^- is a good bridging ligand and that Cr^{2+} reduction of the hydroxo complexes is inner-sphere (*i.s.*).

In monatomic bridges, the function of the bridging ligand can only be to increase the probability of e transfer by tunneling.

Remote Attack. Table 11.28's information on reduction of thiocyanato and azido complexes raises several interesting points. First, notice that all the products are consistent with transfer of the bridging group in an *i.s.* mechanism. Another feature is the fact that lone pairs for bridging are not always available on the atom adjacent to the oxidant. Thus, for example, the only site available for bridging in $[\text{Co}(\text{NH}_3)_5\text{NCS}]^{2+}$ is on S remote from the metal center. The product, CrSCN^{2+} , indicates that remote attack occurs on S. Of course, the symmetry of the azido ligand makes such a distinction experimentally impossible without isotopic labeling. However, drawing the Lewis structure will show that only the remote N can act as a bridge. In $[\text{Co}(\text{SCN})(\text{NH}_3)_5]^{2+}$, both adjacent and remote attack occur. On standing, the CrSCN^{2+} product rearranges to the more stable CrNCS^{2+} isomer. Because Cr^{2+} is a hard acid, it prefers to bond with hard N. This preference is reflected in a lesser stability of the $\text{Cr}-\text{SCN}-\text{Co}$ precursor and accounts for the rate differences between *S*- and *N*-bonded complexes.⁶¹ In general, N_3^- is a better bridging ligand than $\text{M}-\text{NCS}$, and a difference in rates of $\sim 10^4$ for inner-sphere reactions is common. If comparable azido and *N*-bonded thiocyanato complexes are reduced by the same reagent at comparable rates, the reaction is probably outer-sphere. Finally, these data show that electron transfer can occur through a multiatom bridge.

Table 11.28 Rate constants for some redox reactions at 25°C

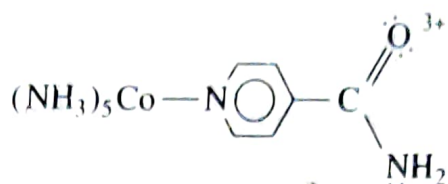
| Oxidant | Reductant | $k(\text{M}^{-1} \text{sec}^{-1})$ | Mechanism |
|---|-----------------------------------|------------------------------------|----------------------|
| $[\text{Co}(\text{NH}_3)_5(\text{H}_2\text{O})]^{3+}$ | Cr^{2+} | ≤ 0.1 | Probably <i>o.s.</i> |
| $[\text{Co}(\text{NH}_3)_5(\text{OH})]^{2+}$ | Cr^{2+} | 1.5×10^6 | <i>i.s.</i> |
| $[\text{Co}(\text{NH}_3)_5(\text{H}_2\text{O})]^{3+}$ | $[\text{Ru}(\text{NH}_3)_6]^{2+}$ | 3.0 | <i>o.s.</i> |
| $[\text{Co}(\text{NH}_3)_5(\text{OH})]^{2+}$ | $[\text{Ru}(\text{NH}_3)_6]^{2+}$ | 0.04 | <i>o.s.</i> |

| Reaction | Product | $k(\text{M}^{-1} \text{s}^{-1})$ |
|--|---|----------------------------------|
| $[\text{Co}(\text{NH}_3)_5\text{NCS}]^{2+} + \text{Cr}^{2+}$ | CrSCN^{2-} | 19 |
| $[\text{Co}(\text{NH}_3)_5\text{N}_3]^{2+} + \text{Cr}^{2+}$ | CrN_3^+ | 3×10^5 |
| $[\text{Co}(\text{NH}_3)_5\text{SCN}]^{2+} + \text{Cr}^{2+}$ | 71% CrNCS^{2+} + 29% CrSCN^{2+} | 1.9×10^5 |

^aFrom the work of Haim, Linck, Taube, Endicott, and others.

⁶¹Sulfur seems to be an especially good mediator of electron transfer. Thus, attack at S sites often occurs kinetically, even when the product is not the most thermodynamically stable one.

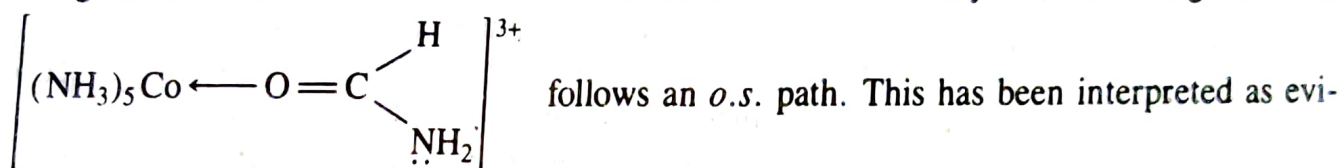
One such electron transfer invokes remote attack by Cr^{2+} on O in



The electron pair on N apparently is not sufficiently basic to provide a site for attack. This seems to be a general feature of $-\text{NH}_2$ groups. Whereas $\left[(\text{NH}_3)_5\text{Co} \leftarrow \text{NH}_2\text{CH} \right]^{3+}$ un-

O

dergoes reduction with Cr^{2+} via remote attack on the carbonyl O, its linkage isomer,



dence that, in remote attack, the oxidant and reductant must belong to a conjugated system involving the bridging ligand. The function of the bridging ligand is to couple the metal orbitals. This is termed the **resonance mechanism** for electron transfer.

The Chemical Mechanism.⁶² Organic bridging ligands having conjugated π -systems display further interesting effects on redox chemistry. A study of the Cr^{2+} reduction of $\left[(\text{NH}_3)_5\text{Co}-\text{C}(\text{O})-\text{C}_6\text{H}_4-\text{C}(\text{O})\text{H} \right]^{2+}$ shows that remote attack occurs on the carbonyl O and gives Co^{2+} as the product. However, $\left[(\text{NH}_3)_5\text{Co}-\text{C}(\text{O})-\text{C}_6\text{H}_4-\text{NO}_2 \right]^{3+}$ gives no Co^{2+} on reduction. Instead, the nitro group on the ligand is reduced. The Cr^{2+} reduction of $\left[(\text{NH}_3)_5\text{Co}-\text{OC}(\text{O})-\text{C}_5\text{H}_4\text{N}_2 \right]^{2+}$ has been found to involve two detectable intermediates. The first decays to give the successor complex, which then affords Co^{2+} as the product.⁶³ Apparently, when the organic ligand is reducible to a fairly stable radical, electron transfer can first reduce the bridging ligand, which then may or may not in turn reduce the other metal. This mode of electron transfer [Mechanism (11.49)] is called the **chemical or radical-ion mechanism**.

